

1 **Title: Chemiomics: Network Reconstruction and Kinetics of Port Wine**  
2 **Aging.**

3

4 Ana Rita Monforte<sup>a</sup>, Dan Jacobson<sup>b</sup>, A. C. Silva Ferreira<sup>a,b</sup>

5 <sup>a</sup> CBQF – Centro de Biotecnologia e Química Fina – Laboratório Associado,  
6 Escola Superior de Biotecnologia, Universidade Católica Portuguesa/Porto,  
7 Rua Arquiteto Lobão Vital, Apartado 2511, 4202-401 Porto, Portugal.

8 <sup>b</sup> IWBT – DVO University of Stellenbosch, Private Bag XI, Matieland 7602,  
9 South Africa.

10

11

12

13

14 Corresponding author: António Silva Ferreira

15 Phone: +351 22 558 0001

16 Fax: +351 22 509 0351

17 E-mail address: asferreira@porto.ucp.pt

18

19

20

21

22

23

24 Running title: Chemiomics: Network Reconstruction and Kinetics of Port Wine

25 Aging.

26 **Abstract**

27 Network reconstruction (NR) has proven to be useful in the detection  
28 and visualization of relationships between the compounds present in a Port  
29 wine aging dataset. This view of the data provides a considerable amount of  
30 information with which to understand the kinetic contexts of the molecules  
31 represented by peaks in each chromatogram. The aim of this study was to use  
32 NR together with the determination of kinetic parameters to extract more  
33 information about the mechanisms involved in Port wine aging. The volatile  
34 compounds present in samples of Port wines spanning 128 years in age were  
35 measured with the use of GC-MS. After chromatogram alignment a peak  
36 matrix was created and all peak vectors compared to one another to  
37 determine their Pearson correlations over time. A correlation network was  
38 created and filtered based on the resulting correlation values. Some nodes in  
39 the network were further studied in experiments on Port wines stored under  
40 different conditions of oxygen and temperature in order to determine their  
41 kinetic parameters. The resulting network can be divided into three main  
42 branches. One is related to compounds that do not directly correlate to age,  
43 the second branch contains compounds affected by temperature and the third  
44 branch contains compounds associated with oxygen. Compounds clustered in  
45 the same branch of the network have similar expression patterns over time;  
46 the same kinetic order and are thus likely to be dependent on the same  
47 technological parameters. Network construction and visualization provides  
48 more information with which to understand the probable kinetic contexts of the  
49 molecules represented by peaks in each chromatogram. The approach  
50 described here is a powerful tool for the study of mechanisms and kinetics in

51 complex systems and should aid in the understanding and monitoring of wine  
52 quality.

53 **Keywords:** Network reconstruction, kinetic parameters, aging, oxygen and  
54 temperature.

55

## 56 **Introduction**

57 Port wine is a fortified wine produced in a specific area in Northern Portugal  
58 known as the Douro region. The diversity of styles offered by Port wines  
59 accounts for its uniqueness among other fortified wines and contributes to its  
60 recognition around the world. Its remarkable ageing potential means that Port  
61 improves in the cask or bottle for much longer than is the case for most wines.  
62 This process implies a significant financial cost that must be recovered in the  
63 final price of the wine. For this reason, it is of commercial interest to have the  
64 maximum amount of information regarding the chemical “fingerprint” for a  
65 given age category resulting from the chemical reactions that take place  
66 during the process and their dependence on technological parameters.

67 Kinetic studies in forced aged Port wine prove the existence of compounds  
68 dependent on temperature (2-furfural, 5-methylfurfural and  
69 hydroxymethylfurfural), oxygen (*cis* and *trans* dioxanes) and on both  
70 parameters (sotolon).<sup>1</sup> However, for a holistic vision of the process it is  
71 necessary to collect a considerable amount of information about other  
72 compounds.

73 In recent years the concept of biological/chemical “fingerprints” has emerged  
74 and comprehensive “omics” technologies (transcriptomics, proteomics and  
75 metabolomics) have become a new way of addressing complex systems.<sup>2</sup>

76 Metabolomics is defined as the study of “as many small metabolites as  
77 possible” in a system.<sup>3</sup> High-throughput metabolomics have the potential to  
78 identify the functional consequences of induced and natural metabolite  
79 variation. However, the data obtained in metabolomics is highly multivariate  
80 and multi scale and thus the use of multivariate analysis techniques are

81 required in order to find trends and/or significant information (biomarkers) in  
82 the data.

83 Network reconstruction has proven to be useful in visualizing the  
84 relationships between all the compounds present in a dataset and the  
85 changes in their concentration over time.<sup>4</sup> This view of the data provides more  
86 information with which to understand the kinetic context of the molecules  
87 represented by peaks in each chromatogram and in doing so facilitates the  
88 identification of candidates for further study.

89 The aim of this study is to use network reconstruction and kinetic parameters  
90 in order to extract more information related to ageing mechanisms and  
91 consequently their dependence on technological parameters such as oxygen  
92 and temperature in order to better explain the chemical “fingerprint” for a  
93 given port wine category. In order to achieve this, old Port wines (age  
94 between 1-129 years) were analyzed by GC-MS and a network constructed  
95 from the peaks found in the total ion current (TIC). Some nodes of the network  
96 were subsequently identified and quantified in forced aged wines (wines  
97 stored on different conditions of oxygen and temperature) to determine their  
98 kinetic parameters

99

## 100 **Material and Methods**

### 101 *Reagents*

102 Chemicals and standards were obtained from Sigma-Aldrich, USA (a high-  
103 purity grade, >99.0%). Dichloromethane and anhydrous sodium sulfate were  
104 obtained from Merck, Darmstadt, Germany.

105

106 *Wine Material*

107 Thirty-four samples of Port wine with ages between 1 and 129 years were  
108 used. All wines were matured in oak barrels and were made following the  
109 standard traditional winemaking procedures for Port wine. For the isothermal  
110 protocol 16 liters of Port wine made on the year of the experiment (without  
111 any oak contact) with pH = 3.4, an amount of dissolved oxygen of 2.5 mg/L, a  
112 free SO<sub>2</sub> level of 17 mg/L, 105 g/L of reducing sugars and 20.5% alcohol  
113 were used in order to determine kinetic parameters.

114

115 *Isothermal Protocol*

116 Kinetics for each compound detected in Port wine were followed using an  
117 isothermal storage method in order to determine the effects of oxygen and  
118 temperature. Isothermal storage was performed at different temperatures (20,  
119 30, 35 and 40°C) and a series of sequential oxygen saturations inside a  
120 hermetically sealed vessel (0 to 10 saturations). Oxygen treatments included  
121 0 (F1), 3 (F2), 5 (F3) and 10 (F4) saturations. Each combination of  
122 oxygen/temperature was performed in glass vessels containing 500 mL of  
123 wine. Oxygen saturation was achieved by stirring the sample for roughly 1  
124 hour until an oxygen concentration of about 8-9 mg/L was reached. The F1  
125 group was never supplemented with O<sub>2</sub>. F2 was saturated on day 14, 35 and  
126 56. F3 was saturated in the beginning of the experiment and at days 14, 28,  
127 42 and 56. F4 was saturated with O<sub>2</sub> on days 0, 14, 21, 28, 35, 42, 49, 56 and  
128 63.

129 This forced aging protocol was performed in duplicate. For logistical reasons  
130 not all samples were analyzed by GC-MS but the replicate was rather used as  
131 a crosscheck procedure.

132

### 133 *Dissolved Oxygen Measurements*

134 Oxygen concentrations were measured using a Fibox 3 LCD fiber optic  
135 oxygen transmitter, a polymer optical fiber and planar oxygen sensitive spots  
136 (5mm sensor spots PSt3), from PreSens Precision Sensing GmbH  
137 (Germany). The sensor was positioned in the center of the vessel (500 mL)  
138 where it remained in contact with the wine at all times.

139

### 140 *Chemical Analysis*

141 The extraction procedure was based on the one described by Silva Ferreira *et*  
142 *al.*<sup>5</sup> Briefly, 50 mL samples of Port were spiked with 50  $\mu$ L of 3-octanol in a  
143 hydro alcoholic solution (1:1, v/v) at 427 mg/L as the internal standard and 5 g  
144 of anhydrous sodium sulphate. The wine was extracted twice with 5 mL of  
145 dicloromethane. The two organic phases obtained were blended and dried  
146 over anhydrous sodium sulphate. Two milliliters of this organic extract was  
147 concentrated to 0.4 mL under a nitrogen stream.

148

### 149 *GC-MS Analysis*

150 Extracts were analyzed using a Varian 450 gas chromatograph, equipped with  
151 a mass detector using Varian 240-MS and Saturn GC-MS workstation  
152 software version 5.51. The injector port was heated to 220 °C. The split vent  
153 was opened after 30 s. The carrier gas was helium C-60 (Gasin, Portugal), at

154 1 mL/min, constant flow. The oven temperature was 40 °C (for 1 min), then  
155 increased at 2 °C/min to 220 °C, and held for 30 min. All mass spectra were  
156 acquired in the electron impact (EI) mode. The ion trap temperatures were  
157 230, 45 and 170 °C. The mass range was m/z 33-350, with a scan rate of 6  
158 scans/s. The emission current was 50 µA, and the electron multiplier was set  
159 in relative mode to autotune procedure. The maximum ionization time was  
160 25000 µs, with an ionization storage level of m/z 35. The injection volume was  
161 1 µL, and the analysis was performed in full-scan mode. Compound  
162 identification was achieved from comparisons of mass spectra obtained from  
163 the sample with those from pure standards injected in the same conditions by  
164 comparing the Kovats indices and the mass spectra present in NIST 05 MS  
165 Library Database.

166

#### 167 *Statistical Analysis*

168 Statistical analysis and the developed methodology involving the experimental  
169 data were performed with R 2.12.1 for Mac, using the following packages: i)  
170 classical multivariate analysis library (mva); ii) main library of Venables and  
171 Ripley's (MASS); iii) Harrell miscellaneous (Hmisc); and iv) R-base packages  
172 (R-Project, 2012).

173

#### 174 *Data Pre-processing*

175 The ASCII file of chromatographic data obtained from each sample was  
176 extracted and a matrix created containing all of the chromatograms. The  
177 intensities were normalized by dividing each value by the intensity of the  
178 internal standard (3-octanol). All of the m/z channels were summed to yield a



179 total ion current (TIC) chromatogram for each sample. The resulting dataset  
180 was then imported into The Unscrambler<sup>®</sup>X 10.1 (Camo, Sweden), where the  
181 first stage of the alignment of chromatograms was performed using  
182 Correlation Optimized Warping (COW).<sup>6</sup> The saturated peaks were then  
183 removed and the baseline corrected. The resulting matrix (GC-MS-TIC matrix  
184 ) was then used for multivariate data analysis as described in the statistical  
185 analysis section.

186

### 187 **Kinetic Network Reconstruction.**

188 In order to attempt to reconstruct the underlying kinetic network, the  
189 fingerprint needed to be further compressed to a single value for each  
190 putative molecule detected by GC-MS. Thus, each chromatographic peak  
191 needed to be replaced with a single value for the intensity and retention-time,  
192 at the apex of each peak and therefore a more refined alignment procedure  
193 was required. This was achieved as follows: An “average chromatogram” was  
194 created by taking the mean of the values at each elution point in the GC-MS-  
195 TIC matrix. The wavelet method of Du et al.,<sup>7</sup> which was originally developed  
196 for peak calling in peptide mass-spec data, was adapted for finding peak  
197 centres in chromatographic data and a Mexican hat wavelet used to  
198 determine the location of all of the peaks in the average and sample  
199 chromatograms. A custom built Perl program was integrated with the R-  
200 based wavelet method to achieve this. The distances between the locations of  
201 all of the peaks in each sample chromatogram and the locations of the peaks  
202 in the average chromatogram were calculated. It was observed that there was  
203 a correlation between peak height and the amount of peak centre shift that

204 occurred across chromatograms and we thus devised a two-step process for  
205 aligning sample peaks to those of the average chromatogram. If the (internal-  
206 standard-normalized) height of the average peak was greater than 2 and the  
207 distance to the nearest sample peak was less than 0.3 minutes then the  
208 intensity value of the sample peak was assigned as the sample value at the  
209 average peak location. However, if the (internal-standard-normalized) height  
210 of the average peak was less than 2 and the distance to the nearest sample  
211 peak was less than 0.15 minutes then the intensity value of the sample peak  
212 was assigned as the sample value at the average peak retention time. This  
213 algorithm was implemented in Perl.

214 As a result of this process a new matrix was created that contained the  
215 retention time of all peaks in the average chromatogram and the intensity  
216 values of all of the peak centres from each sample aligned to these average  
217 retention times. Thus a vector was created for each peak (presumably  
218 representing a compound) across all samples. An all-against-all comparison  
219 was done calculating the Pearson correlation between each and every peak  
220 vector. As such, one is able to track the increase or decrease of compounds  
221 (peaks) during the aging process and determine the correlative relationships  
222 amongst them. We applied a Pearson correlation threshold of 0.8 and  
223 represented the remaining relationships as a mathematical graph in order to  
224 form a correlation network with the nodes representing peaks and the edges  
225 weighted with the Pearson correlations between the peak vectors. In order to  
226 reconstruct the most likely kinetic network underlying the set of chemical  
227 reactions involved in the aging process, a maximum spanning tree was  
228 created by transforming the edge weights into inverse correlations (by taking

229 the difference between the number 1 and the absolute correlation values) and  
230 the subsequent use of a minimum spanning tree (mst) algorithm<sup>8</sup> on the this  
231 inverse correlation network. A minimum spanning tree represents the  
232 shortest possible path through a graph and, as such, selects for the smallest  
233 inverse correlation (i.e highest correlation) pairs between all nodes in the  
234 network. The resulting networks were visualized in Cytoscape.<sup>9</sup>

235

### 236 *Kinetic Parameters*

237 Non-linear regression for model fitting was performed on all data, using a one-  
238 step methodology<sup>10</sup> by maximizing the likelihood function for all temperatures  
239 and using bootstrap sampling to estimate the prediction residuals sum of  
240 squares (PRESS) criterion.<sup>11,12</sup> The lack of fit test was performed to  
241 determine the adequacy of the regression model, and the studentised effect  
242 was studied at a 5% confidence level.

243 The general rate law for compound formation is:

$$r = \frac{d [\text{compound}]}{dt} = k_{obs} [\text{compound}]$$

244 Most of the kinetic models reported in the literature to describe the kinetics of  
245 compound formation are zero-, first- or second-order reaction models.

$$C = C_0 + kt \quad (\text{zero - order})$$

$$C = C_0 \exp kt \quad (\text{first - order})$$

$$\frac{1}{C} = \frac{1}{C_0} + kt \quad (\text{second - order})$$

246 where  $C_0$  is the initial compound concentration,  $t$  the time and  $k$  the kinetic  
247 rate.

248 Therefore the kinetic rate may follow the Arrhenius behavior with temperature.

$$k_{app} = k_{ref} \exp \left[ -\frac{E_a}{R} \left( \frac{1}{T} - \frac{1}{T_{ref}} \right) \right]$$

249 where  $k_{ref}$  ( $\text{day}^{-1}$ ) is the kinetic rate at the reference temperature  $T_{ref}$  (K),  $E_a$   
250 represents the Arrhenius activation energy ( $\text{J mol}^{-1}$ ), and  $R$  is the universal  
251 gas constant ( $\text{J mol}^{-1} \text{K}^{-1}$ ).

252 It was assumed that the studied compounds tend to follow first-order  
253 kinetics<sup>13</sup>

$$C(t) = C_0 + k_{ref} \exp \left[ -\frac{E_a}{R} \left( \frac{1}{T} - \frac{1}{T_{ref}} \right) t \right]$$

254 Statistical analysis and the developed methodology involving the experimental  
255 data were performed with R 2.12.1 for MAC using R-base packages (R-  
256 Project).

257

## 258 **Results and Discussion**

259 Figure 1 shows the network derived from the correlation between all peaks, it  
260 is possible to observe three main branches indicated as A, B and C.

261 It was observed that branch A (Figure 2) included compounds such as  
262 hexanoic (1886), octanoic (2110) and decanoic (2308) acids, which cluster  
263 together. The nodes are colored in shades of red representing increasing  
264 concentration and blue representing decreasing concentration.

265 The ANOVA analysis on perturbed wines shows that acids are not dependent  
266 on temperature or oxygen.

267 In fact its concentration during wine ageing is regulated by the  
268 esterification/hydrolysis between the acid and the correspondent ester, acids  
269 may be formed due to hydrolysis, be lost through chemical esterification, or  
270 remain at a near constant equilibrium concentration depending on their initial,

271 post-fermentation levels.<sup>14</sup> When the system is in balance, there is a constant  
272 correlation between the concentrations of the substances present, governed  
273 by the mass action law.

274 Branch B (Figure 3) contains two compounds that are demonstrated to be  
275 highly sensitive to temperature due to their high activation energy (HMF  
276 (2506) and furfural (1446)), which suggests that the other compounds in the  
277 branch may also be sensitive to temperature.

278 A summary of the ANOVA analysis results is present on each figure as well  
279 as the time expression of each compound identified. All the compounds  
280 identified tend to increase during ageing and ANOVA shows that significant  
281 differences were established across the temperature conditions, meaning that  
282 the compounds identified were all dependent on temperature.

283 It is possible to observe three sub-branches apparently related to activation  
284 energy value. The branch of vanillin (2541),  $\gamma$ -ethoxycarbonyl- $\gamma$ -butyrolactone  
285 (2207), diethyl tartrate (2361) and triethyl citrate (2480) have an  $E_a$  between  
286 16 and 36 kJ/mol.

287 The organic acids esters, diethyl tartrate (2361) and triethyl citrate (2480),  
288 tend to increase due to the high concentration of the respective acids (tartaric  
289 and citric acids), by the reaction between the acid and the ethanol  
290 (esterification reaction). According to Ribéreau-Gayon and Peynaud<sup>14</sup>  
291 polyprotic acids such as tartaric, citric and malic acid esterified more rapidly  
292 than the monoprotic acids acetic, propanoic and butanoic acid and  
293 temperature accelerates the reaction.

294 The  $\gamma$ -ethoxycarbonyl- $\gamma$ -butyrolactone (2207) is a lactone that probably results  
295 from glutamic acid or related compounds, and is dependent on wine ageing

296 and contributes a cherry aroma to wine.<sup>15</sup> The formation of the lactone is an  
297 esterification reaction. Vanillin (2541) is a phenolic aldehyde related with  
298 barrel ageing. Its sensitivity to temperature in wines that were not subject to  
299 wood contact is still unknown.

300 Diethyl glutarate (2392) and ethyl-2-furoate (1525) are located in a second  
301 sub branch. These two compounds have activation energies of 74 and 56  
302 kJ/mol which is higher than those present in the posterior sub-branch. Ethyl-2-  
303 furoate (1525) is also dependent on temperature and its formation is related to  
304 the Maillard reaction.

305 In summary, this branch contains compounds related to temperature and it  
306 would appear that there is an association between network location and  
307 activation energy values.

308 Branch C (Figure 4) contains compounds related to oxidation such as  
309 benzaldehyde (1508) (formed by the oxidation of benzyl alcohol) and  
310 dioxanes (1486 and 1863) and dioxolanes (1619) (formed by the reaction of  
311 ethanal and glycerol). One region of this branch, as shown in Figure 3.6.3.4,  
312 seems to indicate a correlation between sotolon (2232) and 3-hydroxy-2-  
313 methyl-4H-pyran-4-one (1996) (maltol). These two compounds have  
314 somewhat similar chemical structures, i.e. a furanone and a pyranone  
315 respectively and both have a very sweet aroma, normally classified in the  
316 same group of aromas with flavors of “burnt sugar, caramel and maple”.  
317 However, the sensorial impact of each compound are at different orders of  
318 magnitude, ppb for sotolon and ppm for maltol.

319 Sotolon is dependent on temperature and oxygen which suggests that maltol  
320 is dependent on the same parameters and, in fact, the ANOVA analysis

321 indicates that the compound is sensitive to both parameters and has a very  
322 high activation energy when compared to sotolon. This suggests that maltol is  
323 much more sensitive to temperature than is sotolon.

324 Yaylayan et al observed that maltol formation is related with 1-deoxyosone,  
325 an important intermediary of the Maillard reaction.<sup>16</sup> However, there are no  
326 studies on the impact of oxidation on its formation.

327 Other compounds present in this sub-branch (indicated in Figure 4. as  
328 C.1.) of the network appear to be connected with sotolon and maltol. These  
329 compounds are probably dependent on oxygen and temperature and their  
330 identification could be useful in the unraveling of the connection between the  
331 Maillard mechanism and oxidation.

332 These observations would seem to validate the assumptions made that  
333 compounds grouped on the same branch of the network have the same time  
334 expression and consequently the same kinetic order. It was also observed  
335 that compounds grouped together are sensitive to the same technological  
336 parameter.

337 We believe that this network-driven approach to the study of large kinetic  
338 systems is proving to be a useful tool for identifying putative compounds of  
339 interest and to do mechanistic hypothesis generation which can subsequently  
340 be tested experimentally. We would recommend that this type of Chemiomics  
341 approach become a standard workflow for the future investigation of complex  
342 chemical systems.

343

344 **Acknowledgments**

345 This research was funded by the project “Wine Metrics: Revealing the Volatile  
346 Molecular Feature Responsible for the Wine Like Aroma a Critical Task  
347 Toward the Wine Quality Definition.” (PTDC/AGR-ALI/121062/2010) and  
348 partially supported by ESB/UCP plurianual funds through the POS-  
349 Conhecimento Program that includes FEDER funds through the program  
350 COMPETE (Programa Operacional Factores de Competitividade) by national  
351 funds through FCT (Fundação para a Ciência e a Tecnologia), the Wine  
352 Industry Network of Expertise and Technology (Winetech IWBT BI 13/01)  
353 and the Technology and Human Resources Programme and the South African  
354 National Science Foundation.

355

356

357

358

359

360

361

362

363

364

365

366

367

368

369



370 **References**

- 371 1. Martins, R. C.; Monforte, A. R.; Silva Ferreira, A., Port Wine Oxidation  
372 Management: A Multiparametric Kinetic Approach. *J. Agr. Food Chem.* **2013**,  
373 61 (22), 5371-5379.
- 374 2. Courant, F.; Antignac, J.-P.; Monteau, F.; Le Bizec, B., Metabolomics  
375 as a Potential New Approach for Investigating Human Reproductive  
376 Disorders. *J. Proteome. Res.* **2013**, 12 (6), 2914-2920.
- 377 3. Cevallos-Cevallos, J. M.; Reyes-De-Corcuera, J. I.; Etxeberria, E.;  
378 Danyluk, M. D.; Rodrick, G. E., Metabolomic analysis in food science: a  
379 review. *Trends Food Sci. Tech.* **2009**, 20 (11–12), 557-566.
- 380 4. Jacobson, D.; Monforte, A. R.; Silva Ferreira, A. C., Untangling the  
381 chemistry of Port wine aging with the use of GC-FID, multivariate statistics  
382 and network reconstruction. *J. Agr. Food Chem.* **2013**, 61, 2513-2521.
- 383 5. Silva Ferreira, A. C.; Barbe, J.-C.; Bertrand, A., 3-Hydroxy-4,5-  
384 dimethyl-2(5H)-furanone: A Key Odorant of the Typical Aroma of Oxidative  
385 Aged Port Wine. *J. Agr. Food Chem.* **2003**, 51, 4356-4363.
- 386 6. Gong, F.; Liang, Y.-Z.; Fung, Y.-S.; Chau, F.-T., Correction of retention  
387 time shifts for chromatographic fingerprints of herbal medicines. *J.*  
388 *Chromatogr. A* **2004**, 1029 (1–2), 173-183.
- 389 7. Du, P.; Kibbe, W. A.; Lin, S. M., Improved peak detection in mass  
390 spectrum by incorporating continuous wavelet transform-based pattern  
391 matching. *Bioinformatics* **2006**, 22 (17), 2059-2065.
- 392 8. Dijkstra, E. W., A note on two problems in connection with graphs.  
393 *Numer. Math.* **1959**, 1, 269-271.

- 394 9. Shannon, P.; Markiel, A.; Ozier, O.; Baliga, N. S.; Wang, J. T.;  
395 Ramage, D.; Amin, N.; Schwikowski, B.; Ideker, T., Cytoscape: A Software  
396 Environment for Integrated Models of Biomolecular Interaction Networks.  
397 *Genome Res.* **2003**, 13 (11), 2498-2504.
- 398 10. Arabshahi, A.; Lund, D. B., Considerations in calculating kinetic  
399 parameters from experimental data. *J. Food Process. Eng.* **1985**, 7, 239-251.
- 400 11. Hastie, T.; Tibshirami, R., Discriminant adaptative nearest neighbour  
401 classification. *IEEE T. Pattern Anal.* **1996**, 18, 607-616.
- 402 12. Bates, D. M.; Watts, D. G., Non-linear Regression Analysis and its  
403 Applications. John Wiley & Sons: New York, **1998**.
- 404 13. Baig, S.; Rehman, F., Signal Modeling using Singular Value  
405 Decomposition. In *Advances in Computer, Information, and Systems  
406 Sciences, and Engineering*, Elleithy, K.; Sobh, T.; Mahmood, A.; Iskander, M.;  
407 Karim, M., Eds. Verlag: Netherlands, **2006**; pp 31-37.
- 408 14. Ramney, D.; Ough, C. S., Volatile ester hydrolysis or formation during  
409 storage of model solutions of wines. *J. Agr. Food Chem.* **1980**, 28, 928-934.
- 410 15. Wurz, R. E. M.; Kepner, R. E.; Webb, A. D., The Biosynthesis of  
411 Certain Gamma-Lactones from Glutamic Acid by Film Yeast Activity on the  
412 Surface of Flor Sherry. *Am. J. Enol. Viticult.* **1988**, 39 (3), 234-238.
- 413 16. Yaylayan, V. A.; Mandeville, S., Stereochemical Control of Maltol  
414 Formation in Maillard Reaction. *J. Agr. Food Chem.* **1994**, 42 (3), 771-775.
- 415

## Figure Captions

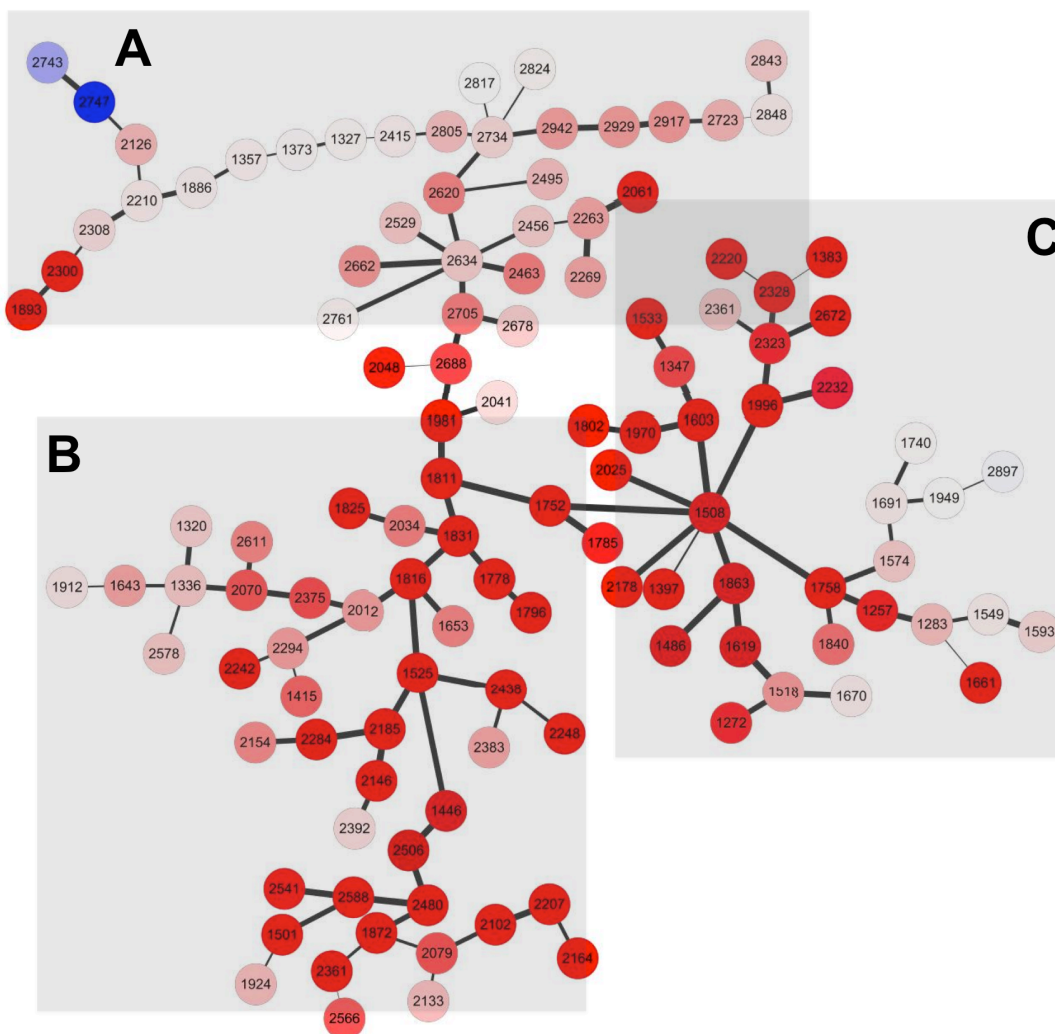
Figure 1. GC-MS Putative Kinetic Network.

Figure 2. Putative Kinetic Network. Branch A Identification: 2210 – Octanoic acid, , 1886– Hexanoic acid, 2308 – Decanoic Acid.

Figure 3. Putative Kinetic Network. Branch B (2070. – pantolactone, 2392 – diethylglutarate, 2541 – vanillin, 2207 -  $\gamma$ -ethoxycarbonyl- $\gamma$ -butyrolactone., 1525 – ethyl furoate.

Figure 4. Putative Kinetic Network. Branch C (2232 – sotolon, 1508 – benzaldehyde, 1486 – cis-5-hydroxy-2-methyl-1,3-dioxane, (1996 – Maltol).

C.1. Sub-branch related with oxygen and temperatur



\ Figure 1. GC-MS Putative Kinetic Network.

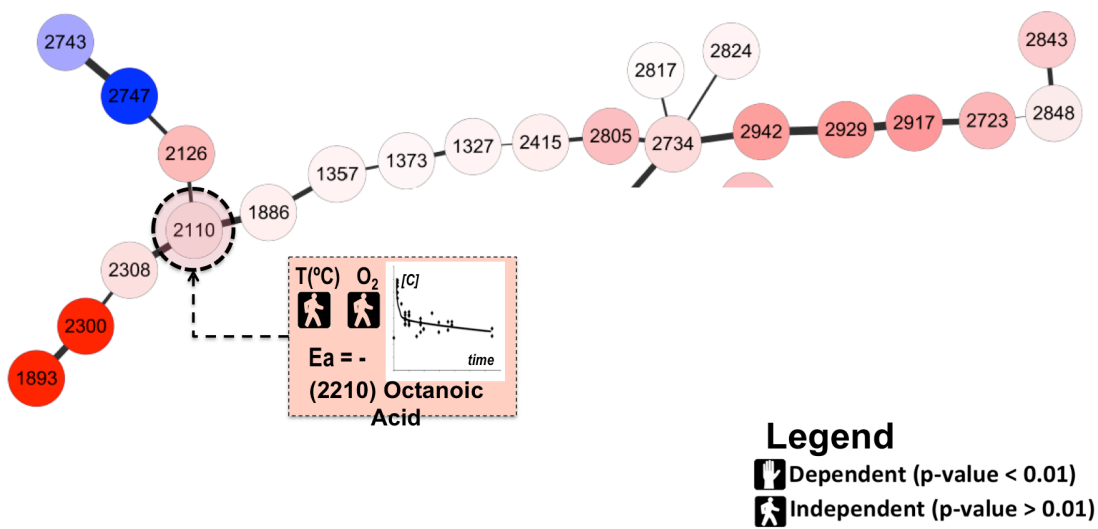


Figure 2. Putative Kinetic Network. Branch A Identification: 2210 – Octanoic acid, , 1886– Hexanoic acid, 2308 – Decanoic Acid.

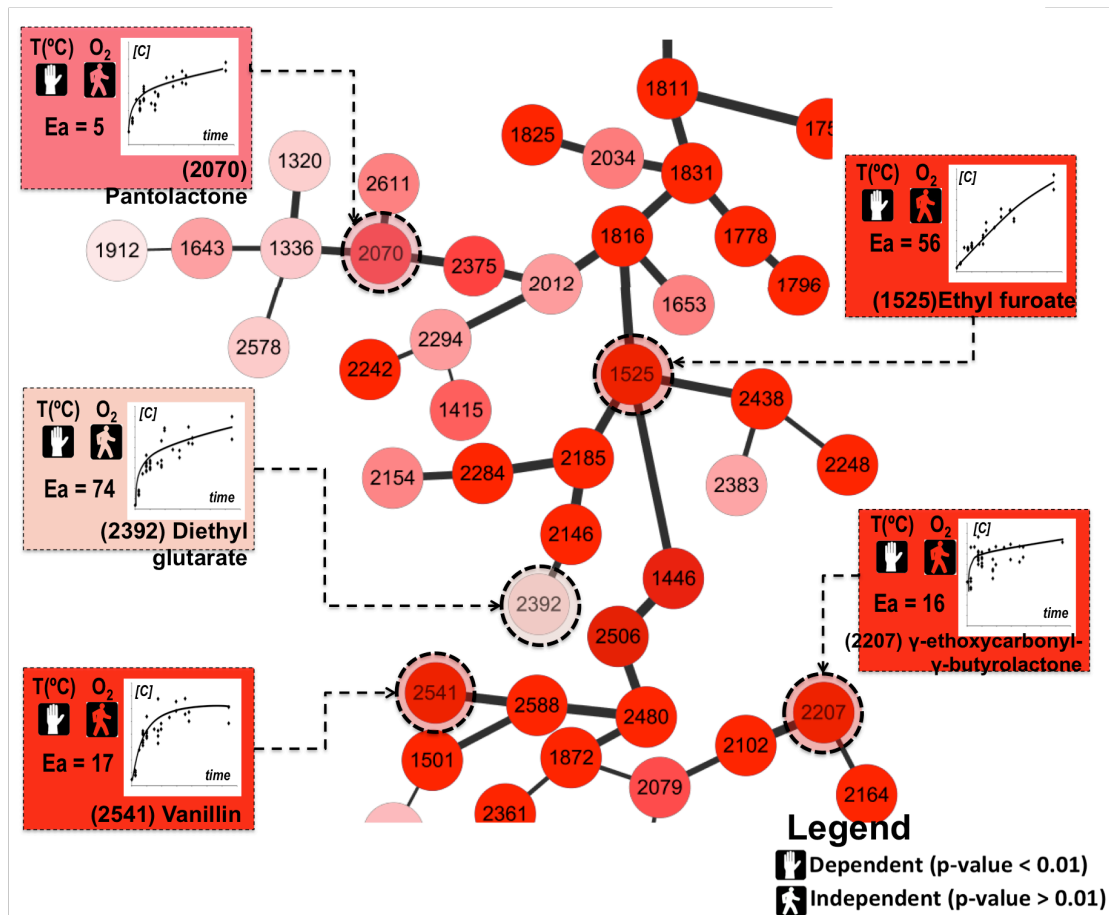


Figure 3. Putative Kinetic Network. Branch B (2070. – pantolactone, 2392 – diethylglutarate, 2541 – vanillin, 2207 -  $\gamma$ -ethoxycarbonyl- $\gamma$ -butyrolactone., 1525 – ethyl furoate.

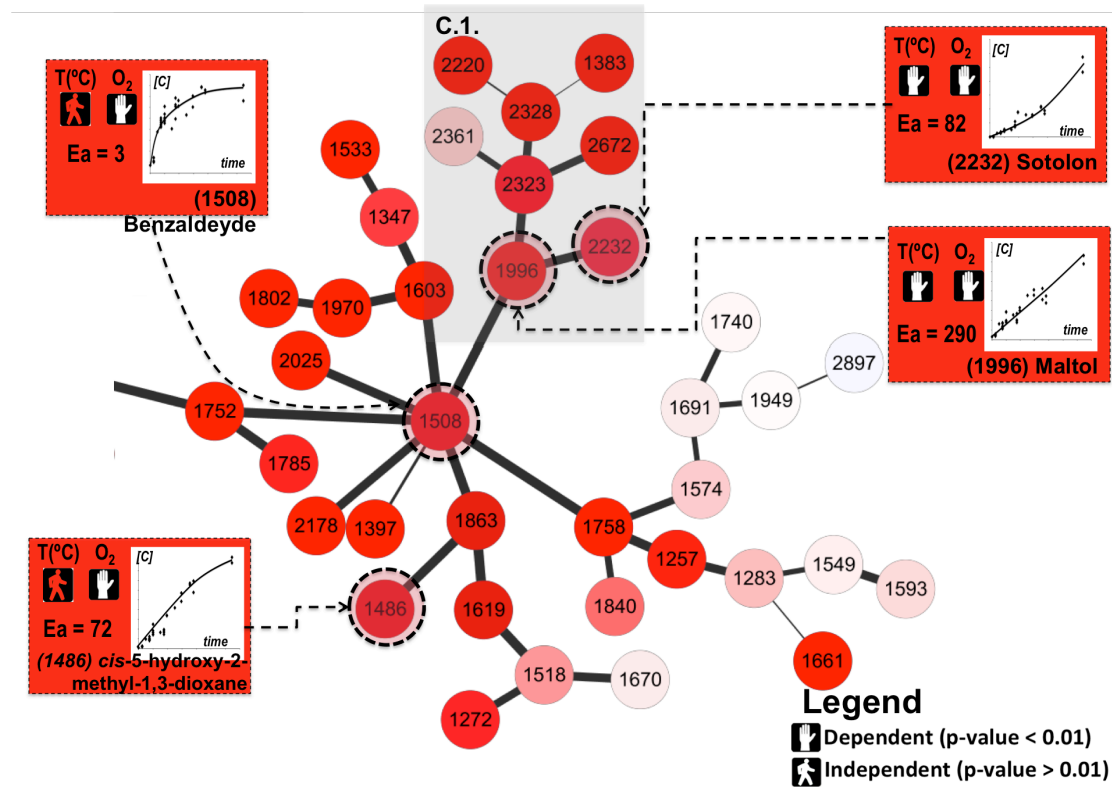
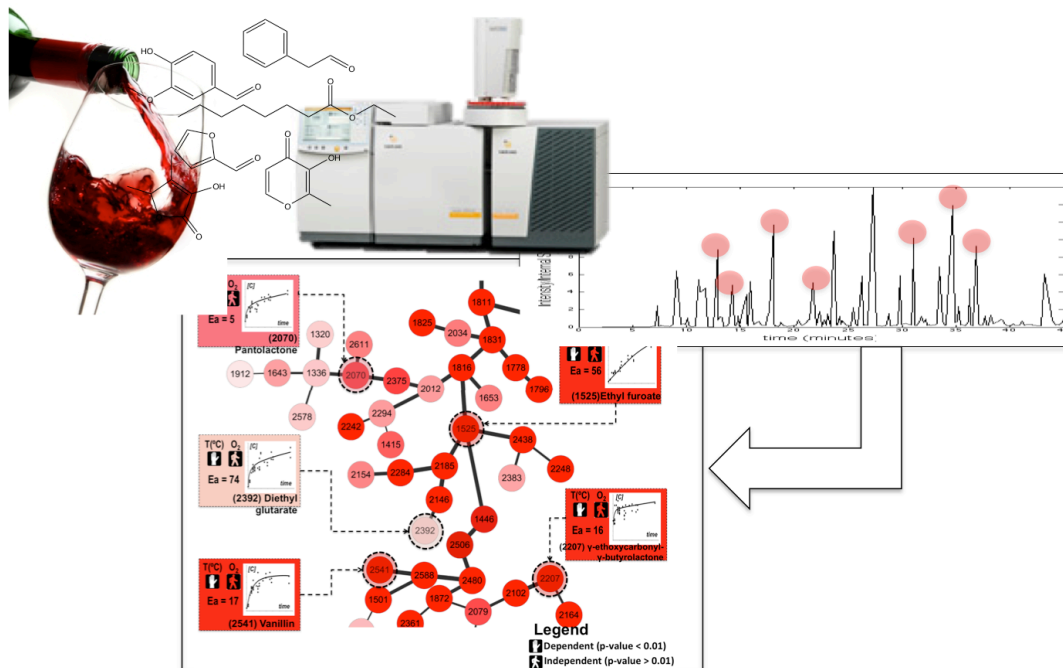


Figure 4. Putative Kinetic Network. Branch C (2232 – sotolon, 1508 – benzaldehyde, 1486 – cis-5-hydroxy-2-methyl-1,3-dioxane, (1996 – Maltol). C.1. Sub-branch related with oxygen and temperature.

## For table of contents only



TOC Graphic